1 Overview of model

1.0.1 The device physical configuration

The side plan of the experiment is as shown:

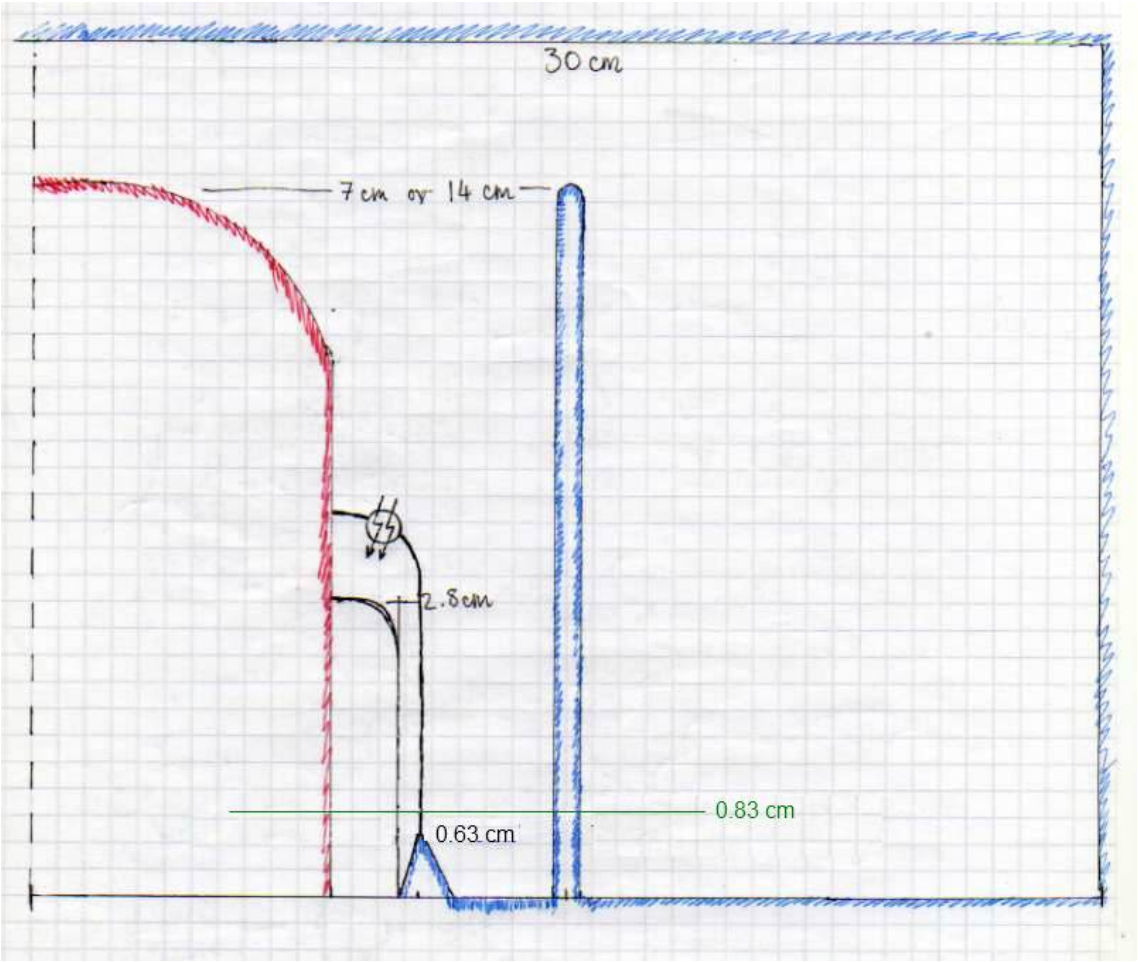

and the plan view is as shown:

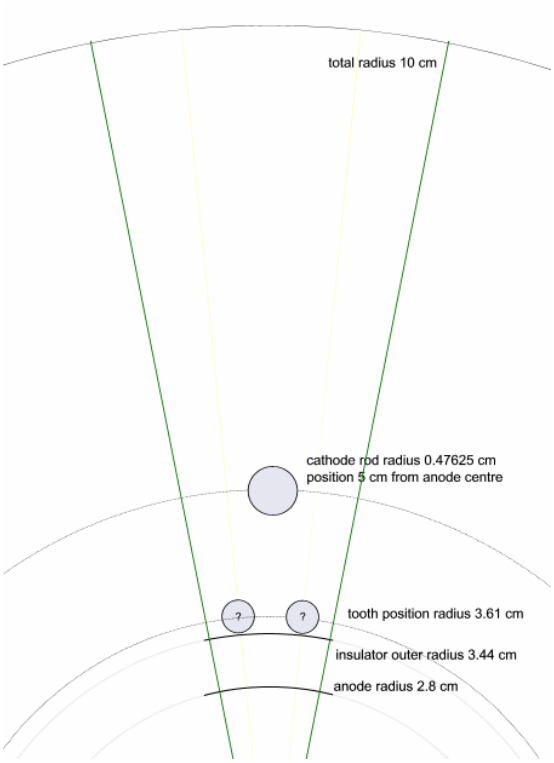

1.0.2 Introduction

This is a 2D simulation of 2 plasma filaments, based on 3 Maxwellian non-MHD fluids, without assuming there is an isotropic thermal or electrical conductivity. The 3 fluids respectively represent all neutral atoms, all singly ionised atoms, and electrons and the fluid dynamic model is constructed largely based on [GZS1977]. There is room for improvement with the number of distribution function moments used, and at least the fully ionised case there is well-known material we have not yet used, such as [EpperleinHaines1986]. Excitations and charge exchange are not yet in the model. We have not yet acquired Zhdanov's book on 3-fluid transport . The model uses centimeter-gram-second units.

We begin with uniform density and about 97% neutral, with the ionisation concentrated above the teeth on the cathode. We seek to simulate for 500-600 nanoseconds to cover the filament formation stage, after which the filaments are becoming more amenable to being modelled analytically.

1.1 The base (fluid dynamic, field evolution) model equations in brief

1.1.1 Preliminary

Define cyclotron frequencies, collision frequencies and some convenient tensors:

electron gyrofrequency	$\omega_{ce} = \frac{eB}{m_e c}$
ion gyrofrequency	$\omega_{ci} = \frac{eB}{m_i c}$
velocity-independent electron-ion collision frequency	$\nu_{ei} = \bar{\nu_{ei}} = \frac{1}{3.44\times10^5} \frac{n_e(\ln\Lambda_e)}{T_e^{3/2}/k_B}$
ion-ion collision frequency	$\nu_{ii} = 2^{-1/2} \frac{1}{2.09\times10^7} \frac{n(\ln\Lambda_{ion})}{T_{\rm ion}^{3/2}/k_B}$
species-neutral coll. freq'cies (η ~ viscosity)	$\nu_{sn}^{\eta} = n_n \sigma_{sn}^{\eta} \left(\frac{T_s}{m_s} + \frac{T_n}{m_n}\right)^{1/2}$
species-neutral coll. freq'cies (MT ~ momentum-transfer)	$\nu_{sn}^{\rm MT} = n_n \sigma_{sn}^{\rm MT} \left(\frac{T_s}{m_s} + \frac{T_n}{m_n}\right)^{1/2}$
Friendly collision frequency for electrons	$\nu_{e\heartsuit} = \nu_{en}^{\eta} + 1.87\bar{\nu_{ei}}$
Friendly collision frequency for ions	$\nu_{i\heartsuit} = \frac{3}{4}\nu_{in}^{\eta} + \frac{4}{5}\nu_{ii} - \frac{1}{4}\frac{\nu_{in}^{\eta}\nu_{ni}^{\eta}}{\left(3\nu_{ni}^{\eta}+\nu_{nn}^{\eta}\right)}$
Convenient Alfven tensor	$\Upsilon_{e\heartsuit} = \Upsilon_{e\heartsuit}^{-} = \Upsilon\left(\nu_{e\heartsuit}, \omega_{ce}\right) = \nu_{e\heartsuit}\left(\nu_{e\heartsuit} - \omega_{ce}\times\right)^{-1}$
Convenient Alfven tensor for ions	$\Upsilon_{i\heartsuit}^{+} = \Upsilon\left(\nu_{i\heartsuit}, \omega_{ci}\right)^{Transpose} = \nu_{i\heartsuit}\left(\nu_{i\heartsuit} + \omega_{ci}\times\right)^{-1}$

1.1.2 Continuity equation

In fluid frame,

$$\frac{\partial n_s}{\partial t} = -n_s \nabla \cdot v_s + \text{net production rate}$$

1.1.3 Fluid accelerations introduction

In the fluid frame:

$$\frac{\partial v_s}{\partial t} = -\frac{1}{n_s m_s}\nabla\left(n_s T_s\right) - \frac{1}{n_s m_s}\nabla\cdot\Pi_s + \frac{Z_s e}{m_s}\left(E + \frac{v_s \times B}{c}\right) + \frac{\delta v_s}{\delta t} \tag{1}$$

where these terms are

Acceleration due to thermal pressure $-\frac{1}{nm}\nabla\left(nT\right)$

Acceleration due to viscous forces $-\frac{1}{nm}\nabla\cdot\Pi$ For ions and electrons we use the viscous stress tensor from [NRLFormulary], whereas for neutrals we use only a momentum diffusion component. The connection between heat conduction and viscous acceleration is noted in [Braginskii1965].

Acceleration due to Lorentz force $\frac{Z_s e}{m_s}\left(E+\frac{v_s\times B}{c}\right)$ Here $Z_e=-1$, $Z_i=1$. e is a positive value.

Rate of change due to collisions $\frac{\delta v_s}{\delta t}$ Where the sum is over other species β,

$$\frac{\delta v_s}{\delta t}=\sum_\beta \frac{\delta v_s}{\delta t}_{s\beta}=-\frac{1}{m_s}\sum_\beta R_{s\beta} \tag{2}$$

Note our definition of R matches [GZS1977], not [NRLFormulary] which is a factor n different.

1.1.4 Fluid acceleration equations therefore are:

In ion fluid frame:

$$\begin{aligned}\frac{\partial v_i}{\partial t} &= -\frac{1}{n_i m_i}\nabla\left(n_i T_i\right)-\frac{1}{n_i m_i}\nabla\cdot\Pi_i+\frac{e}{m_i}E-\omega_{ci}\times v_i\\ &\quad+\left[\text{effect of new ions at } v_n\right]-\frac{m_n}{m_i+m_n}\nu_{in}^{\mathrm{MT}}\left(v_i-v_n\right)\\ &\quad+\frac{3}{2}\frac{\nu_{ie}}{m_i\nu_{e\heartsuit}}\Upsilon_{e\heartsuit}\nabla T_e-\frac{m_e}{m_i}\left(1_{3\times3}-\frac{9}{10}\frac{\nu_{ei}}{\nu_{e\heartsuit}}\Upsilon_{e\heartsuit}\right)\nu_{ie}\left(v_i-v_e\right)\end{aligned} \tag{3}$$

In electron fluid frame:

$$\begin{aligned}\frac{\partial v_e}{\partial t} &= -\frac{1}{n_e m_e}\nabla\left(n_e T_e\right)-\frac{1}{n_e m_e}\nabla\cdot\Pi_e-\frac{e}{m_e}E+\omega_{ce}\times v_e\\ &\quad+\left[\text{effect of new e's at } v_n\right]-\frac{m_n}{m_e+m_n}\nu_{en}^{\mathrm{MT}}\left(v_e-v_n\right)\\ &\quad-\frac{3}{2}\frac{\nu_{ei}}{m\nu_{e\heartsuit}}\Upsilon_{e\heartsuit}\nabla T_e-\left(1_{3\times3}-\frac{9}{10}\frac{\bar{\nu_{ei}}}{\nu_{e\heartsuit}}\Upsilon_{e\heartsuit}\right)\nu_{ei}\left(v_e-v_i\right)\end{aligned} \tag{4}$$

In neutral fluid frame:

$$\begin{aligned}\frac{\partial v_n}{\partial t} &= -\frac{1}{n_n m_n}\nabla\left(n_n T_n\right)-\frac{1}{n_n m_n}\nabla\cdot\Pi_n+\left[\text{effect of new neutrals at } \tfrac{m_i v_i+m_e v_e}{m_n}\right]\\ &\quad-\frac{m_e}{m_e+m_n}\nu_{ne}^{\mathrm{MT}}\left(v_n-v_e\right)-\frac{m_i}{m_i+m_n}\nu_{ni}^{\mathrm{MT}}\left(v_n-v_i\right)\end{aligned} \tag{5}$$

where $\nabla\cdot\Pi_n$ gives rise to isotropic viscosity with no Coulombic part, ie, p_x does not affect p_y.

1.1.5 Temperature evolution introduction:

In the fluid frame,

$$\frac{\partial T_s}{\partial t}=-\frac{2}{3}T_s\nabla\cdot v_s-\frac{2}{3n}\nabla\cdot q_s-\frac{2}{3n}\Pi:\nabla v_s-\frac{2}{3}\sum_\beta\left(\frac{m_s m_\beta}{m_s+m_\beta}\frac{\delta v_s}{\delta t}_{s\beta}\cdot\left(v_s-v_\beta\right)\right)+\frac{\delta T_s}{\delta t} \tag{6}$$

where these terms are

Compressive heating $-\frac{2}{3}T_s\nabla\cdot v_s$

Divergence of heat flux vector $-\frac{2}{3n}\nabla\cdot q_s$ This can give rise to both heat conduction $\frac{2}{3n_s}\nabla\cdot\left(\kappa_s\nabla T_s\right)$ and a thermoelectric drift of heat.

Viscous heating $-\frac{2}{3n}\Pi:\nabla v_s$ This represents the additional thermal energy that cancels the change in directed kinetic energy under viscous momentum flow.

Frictional heating, inc. resistive heating $-\frac{2}{3}\sum_\beta \left(\frac{m_s m_\beta}{m_s+m_\beta}\frac{\delta v_s}{\delta t}_{s\beta}\cdot(v_s-v_\beta)\right)$ This arises due to the change in directed kinetic energy on inter-species momentum transfer.

Inter-species heat transfer effect $\frac{\delta T}{\delta t}$

1.1.6 Temperature evolution equations therefore are:

Ion temperature evolution

Again in the fluid frame:

$$\begin{aligned}\frac{\partial T_i}{\partial t} &= -\frac{2}{3}T_i\nabla\cdot v_i+\frac{2}{3n_i}\nabla\cdot\left(\kappa^{\text{ion}}\nabla T_i\right)-\frac{2}{3n_i}\Pi:\nabla v_i+\frac{2}{3}\frac{m_i m_n^2}{(m_i+m_n)^2}\nu_{in}\left(v_n-v_i\right)^2\\ &\quad+\left[\text{effect of new ions at }\tfrac{T_n}{2}\right]-\sum_{\beta\neq i}\frac{2m_i m_\beta}{(m_i+m_\beta)^2}\nu_{i\beta}^{\text{MT}}\left(T_i-T_\beta\right)\end{aligned}\tag{7}$$

where ion thermal conductivity tensor

$$\kappa^{\text{ion}}=\kappa_\parallel^{\text{ion}}\Upsilon_{i\heartsuit}^{+}=\frac{5}{2}\frac{n_i T_i}{m_i\nu_{i\heartsuit}}\Upsilon_{i\heartsuit}^{+}\tag{8}$$

Electron temperature evolution

$$\frac{\partial T_e}{\partial t} =$$

$$\text{compressive htg}\quad -\frac{2}{3}T_e\nabla\cdot v_e\tag{9}$$

$$\begin{aligned}&\text{heat conduction} && +\frac{2}{3n_e}\nabla\cdot\left(\kappa^e\nabla T_e\right)\\ &\text{viscous htg} && -\frac{2}{3n_e}\Pi:\nabla v_e\\ &\text{thermoelectric heat drift} && -\frac{1}{n_e}\nabla\cdot\left(n_e T_e\frac{\bar{\nu_{ei}}}{\nu_{e\heartsuit}}\Upsilon_{e\heartsuit}\left(v_e-v_i\right)\right)\\ &\text{frictional+resistive} && +\frac{2}{3}\frac{m_e m_n}{m_e+m_n}\nu_{en}\left(v_n-v_e\right)^2-\frac{2}{3}m_e\frac{\delta v_e}{\delta t}_{ei}\cdot\left(v_e-v_i\right)\\ &\text{ionisation-related} && +\left[\text{effect of new e's at }\tfrac{T_n}{2}\right]+\frac{2\text{E}_\infty^0}{3n_e}\left[\text{net ion production rate}\right]\end{aligned}$$

$$\text{inter-species transfer}\quad -\sum_{\beta\neq e}\frac{2m_e m_\beta}{(m_e+m_\beta)^2}\nu_{e\beta}^{\text{MT}}\left(T_e-T_\beta\right)\tag{10}$$

where electron thermal conductivity tensor

$$\kappa^e=\kappa_\parallel^e\Upsilon_{e\heartsuit}=\frac{5}{2}\frac{n_e T_e}{m\nu_{e\heartsuit}}\Upsilon_{e\heartsuit}\tag{11}$$

Neutral temperature evolution

$$\begin{aligned}\frac{\partial T_n}{\partial t} &= -\frac{2}{3}T_n\nabla\cdot v_n+\frac{2}{3n_n}\nabla\cdot\left(\kappa^n\nabla T_n\right)-\frac{2}{3n_n}\Pi:\nabla v_n+\frac{2}{3}\frac{m_i^2 m_n}{(m_i+m_n)^2}\nu_{ni}\left(v_n-v_i\right)^2\\ &\quad+\left[\text{effect of new neutrals at }T_e+T_i\right]-\sum_{\beta\neq n}\frac{2m_n m_\beta}{(m_n+m_\beta)^2}\nu_{n\beta}^{\text{MT}}\left(T_n-T_\beta\right)\end{aligned}\tag{12}$$

where we use a scalar thermal conductivity

$$\kappa_{[\text{GSKB}]}^{\text{neutral}}=10\frac{n_n T_n}{m_n\nu_{n\heartsuit}}$$

1.1.7 Maxwell's equations

$$\nabla \cdot E = 4\pi\rho \qquad \text{[Gauss]} \tag{13}$$

$$\nabla \times E = -\frac{1}{c}\frac{\partial B}{\partial t} \qquad \text{[Faraday]} \tag{14}$$

$$\nabla \cdot B = 0 \tag{15}$$

$$\nabla \times B = \frac{4\pi}{c}J + \frac{1}{c}\frac{\partial E}{\partial t} \qquad \text{[Ampere} - \text{Maxwell]} \tag{16}$$

The boundary conditions for the curl-free part of E include that the circuit current $I_z(t)$ follows a prescribed trajectory. We can regard this as adding a potential gradient E field due to the circuit, which scales according to the voltage and results in the circuit current, or, we can regard it as setting the scalar potential ϕ on the electrodes.

The only additional field other than that is $B_z+ = 2.7$Gauss due to the earth's magnetic field and an electromagnetic coil.

2 Numerical instability timescales

Charge oscillation instability and Faraday's Law instability These are both governed by the plasma frequency. I will describe the second of them. The easiest way to understand it is to consider from below in the full Maxwell case, $\frac{1}{c^2}\frac{\partial^2 A}{\partial t^2} = \nabla^2 A + \frac{4\pi}{c}J$. Look at a simplified system:

$$\frac{\partial J}{\partial t} = \frac{q^2 n}{m}\left(-\frac{1}{c}\frac{\partial A}{\partial t}\right)$$

$$\frac{\partial^2 A}{\partial t^2} = 4\pi c J$$

Hence,

$$\frac{\partial^2 J}{\partial t^2} = -4\pi\frac{q^2 n}{m}J$$

so that for stability of an explicit method we roughly require $h < \left(4\pi\frac{q^2 n}{m}\right)^{-1/2} = (3.2\text{e}9n)^{-1/2}$. The same timestep may apply for charge oscillations.

Thermal pressure instability Consider the simplified system

$$\frac{d}{dt}(\nabla \cdot v) = -\frac{\nabla^2 (nT)}{nm}$$

$$\frac{d}{dt}(nT) = -\frac{5}{3}(nT)(\nabla \cdot v)$$

Heuristically, $\nabla^2 (nT) \sim -\left(nT - (nT)_{surround}\right)/\delta^2$.

Suppose initially we have $nT = (nT)_{surround} + \varepsilon$ for some reason.

Then with an Euler step we would get $\nabla \cdot v = h\varepsilon/nm\delta^2$; then $nT - (nT)_{surround} = \varepsilon\left(1 - \frac{h^2}{\delta^2}\frac{5}{3}T/m\right)$.

For this to be diminishing the size of the aberration, take $h < \delta/\sqrt{T/m}$.

Heat conduction CFL instability This arises when a spike of temperature causes too violent of an outflow of heat, leading to oscillations (which will soon bring about negative temperatures).

Gyroacceleration instability Following electron velocity has a problem if the timestep would see it rotate dramatically: proper treatment of rotating the new additional velocity is needed. Correct displacement is also a problem: we have to infer the average velocity direction over time, which may only be easy in Ohm's Law conditions.

Light propagation instability

To simulate a wave travelling at speed c we expect the CFL timestep to be $\delta/2c$, if we are using the full Maxwell's equations.

2.1 Summary of critical timesteps:

		Initial	Final	
	n_{max}	1e18	1e21	
	T^e_{max}	4.8e-12	4.8e-11	
	δ_{min}	3.2e-3	1e-4	<–Example values
	B_{max}	1e4	1e6	
	$\kappa^e_{max} = 6e20 T^{2.5}_{e[eV]}$	9.4e21	3.0e24	
	$\nu\bar{}_{ei}$	2.3e12	7.3e13	
Critical timesteps:				Comment:
Electron heat conduction	$0.1 n \delta^2 / \kappa^e$	1.1e-10	3.4e-13	Respect; fighting not worth it.
Electron thermal pressure	$\delta / \sqrt{T_e / m_e}$	4.4e-11	4.4e-13	Respect; can fight if necessary.
Electron gyroacceleration	$1/\omega_{ce}$	5.7e-12	5.7e-14	Can overcome with Ohm's or implicit accel
Resistance	$1/\nu\bar{}_{ei}$	4.3e-13	1.4e-14	Can overcome with Ohm's or implicit accel
Light propagation	$\delta / (2c)$	5.3e-14	1.7e-15	Can overcome with Darwin
Plasma period	$1/\sqrt{3.2e9\ n}$	1.8e-14	5.6e-16	Faraday part easy; charge oscillations hard
ES under Maxwell(?)	$\sqrt{\frac{\delta}{c} / \sqrt{\frac{4\pi q^2 n}{m}}}$	4.3e-14	1.4e-15	See below for "remarkable fact"

3 The simulation to date

3.0.1 Lagrangian mesh and remeshing

There are two reasons for using a Lagrangian (moving mesh) simulation, but they both come down to the type of description that an arbitrary mesh can offer.

For development I use 36864 = 144*256 data points; for producing results assume this would be such as 184320 = 720*256. As long as there is no ODE solving, the cost is linear in the number of points; when ODE solving was involved, a near-linear-cost method was in view.

We assume we shall want the inter-data spacing ("cell width") to eventually reach 1 micron or less in some places. If we had instead used 1 micron resolution from the beginning in a fixed mesh, then we need about 2e8 data points. The Lagrangian mesh therefore saves 3 orders of cost in both runtime and memory footprint.

The Lagrangian mesh may also be useful in helping describe sharp, moving fronts in space since we acquire rows of points along the expanding front. At any rate it should give a better description than with a comparable number of points in given positions.

Heuristically, due to the highly collisional fluids, a wavefront will push on the material outside it, so it is reasonable to advect data locations and keep the same amount of mass within regions whose boundaries are advected. In other words, the fluid advection is assumed to be a continuous deformation. This is a different choice than an Eulerian treatment where fluid can catch up with and mix with the next cell's fluid.

Once filaments develop, they may attain a density of 10^{20} up to 10^{21}/cc. If we started with a density of 92160 vertices/cm^2 for $n = 10^{18}$ then at $n = 10^{20}$ we will only have a 10 times decrease in spacing, to give roughly a 3-micron resolution. If we wish to then get higher resolution, then we may have to scatter extra vertices, probably manually, probably removing them from elsewhere.

Mesh maintenance

Since there is an arbitrary set of data positions, we have to decide how data will interact locally. Whatever data will represent, this requires deciding which locations are neighbours, and to this end we have to find a triangulation. It is convenient for this to have the property known as Delaunayhood, ie that each triangle's circumcircle (the circle passing through each of its corners) contains no other data locations. This is maintained by applying exhaustive flips every time the mesh is altered.

3.0.2 Current that maintains quasineutrality is the key problem

It was already possible to run a simulation in which planar current was suppressed and the motion ambipolar. The challenge is to run a simulation in which planar currents are allowed, and hence on to

3D. Currents are challenging.

Suppose we simply allow the curl-free part of the current density J to be incorrect, and say "the departure of n_e from n_{ion} is ignored". Then there are problems with incorrect resistive heating and advection of T_e. In the case of implicit acceleration, there is also the rotation of the false current (basically, normal to the contours of density) into the directions that are allowed (basically, parallel to the contours of density); this means the B field is then also wrong. In the case that under Darwin's approximation, the timestep is greater than a gyroperiod and there is supposedly a way to summarise the relationship between J and E, then at the very least, the E field needs to obey Gauss's Law or the current is again incorrect even in the allowed directions. So in essence, allowing the curl-free part of J to be completely incorrect is a non-starter.

In some circumstances we could proceed by solving for a potential ψ so that adding the potential gradient to J would set $\nabla \cdot J = 0$ while leaving the curl of J unaltered. That the current is divergence-free would be a fair approximation to reality. But the justification for this procedure would have to be very careful, bearing in mind that the *fastest* process is for charge density accumulation to limit the current in certain directions, whereas we would likely be applying this addition to J *after* taking various other limits.

Early on, an approach was tried in which neutrality would be maintained by adding a potential gradient to the E field. This was found to be technically a little more difficult than, actually recognising the existence of a charge density, performing an implicit step for current and charge flow. The assumption of $n_e = n_i$ did not make things any easier.

This ODE-solving approach is now shelved and the present focus is on an evolutionary approach with a short timestep.

3.1 The Darwin, ODE-solving based approach

A considerable effort was spent developing a simulation using Darwin's approximation [Hewett1985, BL91]. This can be shown to arise from taking potentials (ϕ, A) that solve $\nabla^2 A = -\frac{4\pi}{c} J$, $-\nabla^2 \phi - \nabla \cdot \left(\frac{1}{c}\frac{\partial A}{\partial t}\right) = 4\pi\rho$ assuming $B = \nabla \times A$, $E = -\nabla\phi - \frac{1}{c}\frac{\partial A}{\partial t}$. With timestep much higher than the plasma period, this simulation involved an implicit treatment of fields, current and the flow of charge. The current and charge flow are taken as implied by the solution of a 4-dimensional ODE for (ϕ, A) in space (on the arbitrary mesh) at every timestep. A tensor Ohm's Law was used.

Early hopes that this would be achieved by merely updating a previous solution iteratively, were not fulfilled. If you want to evolve the solution in time, you are apparently better off using Maxwell and accepting a short timestep. With a view to solving the ODE more or less afresh each time, I developed a solver based on multigrid and using a Jacobi-Richardson Least Squares at each level, with LU on the coarsest level. The solver is powerful enough that had it always converged, the runtime would be brought down to a manageable amount. There is scope for massive parallelisation, but it never reached that point. In practice it proved very difficult to get such an ODE solver to succeed once the full equations are being used. Possibly by changing to use offset velocity data, we could have got closer to diagonal dominance and made the job of the solver easier.

The solver code is still used to set up the initial profile of current J_z and magnetic potential A_z by making assumptions about an Ohm's Law, and the magnetic potential growth rate: $\left(\left(dA_z/dt\right)/A_z\right)(x) = \left(dI_z/dt\right)/I_z$.

3.2 Lorenz gauge Maxwell evolution

If we use Maxwell's equations instead of Darwin's approximation, there is a change to the nature of the numerical problem of charge oscillations, compared with Darwin.

Faraday's Law and Gauss's Law for Magnetism are satisfied automatically if we again write:

$$E = -\nabla\phi - \frac{1}{c}\frac{\partial A}{\partial t}$$

$$B = \nabla \times A$$

It can be proved that we can obtain Lorenz gauge $\left[\frac{\partial \phi}{\partial t} = -c\nabla \cdot A\right]$ potentials that allow Gauss and

Ampere-Maxwell to be satisfied, by taking

$$\frac{1}{c^2}\frac{\partial^2\phi}{\partial t^2} = \nabla^2\phi + 4\pi\rho \tag{17}$$

$$\frac{1}{c^2}\frac{\partial^2 A}{\partial t^2} = \nabla^2 A + \frac{4\pi}{c}J \tag{18}$$

and satisfying some initial conditions such as $\nabla \cdot E = 4\pi\rho$ and $\nabla^2 A + \frac{4\pi}{c}J = 0$.

3.2.1 Numerical integrators that maintain Gauss's Law and Lorenz gauge

It can be shown that a step maintains Gauss and Lorenz if you take the time-derivative from a source system q that satisfies Gauss and Lorenz. ie:

$$\frac{\partial\phi}{\partial t}_{k+} = \frac{\partial\phi}{\partial t}_{k} + hc^2\left(\nabla^2\phi_q + 4\pi\rho_q\right)$$

$$\phi_{k+} = \phi_k + h\frac{\partial\phi}{\partial t}_{q}$$

$$\frac{\partial A}{\partial t}_{k+} = \frac{\partial A}{\partial t}_{k} + hc^2\left(\nabla^2 A_q + \frac{4\pi}{c}J_q\right)$$

$$A_{k+} = A_k + h\frac{\partial A}{\partial t}_{q}$$

$$\rho_{k+} = \rho_k - h\nabla \cdot J_q$$

It follows that methods such as Explicit Midpoint and RK4 Classic do maintain Gauss and Lorenz. Some other methods (semi-implicit) do not.

3.2.2 An implicit advance to overcome Faraday's instability: Implicit Midpoint Verlet

Introductory version with $J = q\left(n_i v_i - n_e v_e\right)$ instead of v. Some schemes such as Backward Midpoint were investigated but the best result came from applying implicit midpoint for $\left(J, \frac{\partial A}{\partial t}\right)$:

$$\frac{\partial A}{\partial t}_{k+1} = \frac{\partial A}{\partial t}_{k} + hc^2\left(\nabla^2 A_{k+1/2} + \frac{4\pi}{c}\left(\frac{1}{2}J_k + \frac{1}{2}J_{k+1}\right)\right) \tag{19}$$

$$J_{k+1} = J_k + h\left(-\nu + \omega\times\right)\left(\frac{1}{2}J_k + \frac{1}{2}J_{k+1}\right) + h\frac{q^2 n}{m}\left(-\nabla\phi_{k+1/2} - \frac{1}{2c}\left(\frac{\partial A}{\partial t}_{k} + \frac{\partial A}{\partial t}_{k+1}\right)\right) \tag{20}$$

To maintain Gauss and Lorenz it is sufficient to take

$$\frac{\partial\phi}{\partial t}_{k+1/2} = \frac{\partial\phi}{\partial t}_{k} + \frac{h}{2}c^2\left(\nabla^2\phi_k + 4\pi\rho_k\right) \tag{21}$$

$$A_{k+1/2} = A_k + \frac{h}{2}\frac{\partial A}{\partial t}_{k} \tag{22}$$

and

$$4\pi\rho_{k+1} - 4\pi\rho_k = -4\pi h\nabla\cdot\left(\frac{1}{2}J_k + \frac{1}{2}J_{k+1}\right) \tag{23}$$

with the advance of ϕ as midpoint, A trapezoidal.

We shall call this an Implicit Midpoint Verlet scheme (IMV), referring to the well-known Verlet scheme in molecular dynamics, in which one half of a coupled system advances trapezoidally and the other half as midpoint.

3.2.3 A remarkable fact (which would be even more useful if the mass per cell were greater)

A back-of-envelope comparison suggests NOTIONALLY that it is possible that using the IMV scheme can overcome electrostatic oscillations.

For a purely electrostatic case, with A neglected, where $\leftharpoondown$ means "affected by", we would have

$$\rho \leftharpoondown \nabla \cdot J$$

$$\frac{\partial \phi}{\partial t} \leftharpoondown 4\pi c^2 \rho$$

$$\phi \leftharpoondown \frac{\partial \phi}{\partial t}$$

$$J \leftharpoondown \frac{q^2 n}{m} \nabla \phi$$

Now on the face of it here we have a cycle of 4 things and the multiplied factor is $\frac{c^2}{\delta^2} \frac{4\pi q^2 n}{m}$ so it is possible the critical timestep for an explicit method could be on the order of

$$h_{critical} = \left(\frac{c^2}{\delta^2} \frac{4\pi q^2 n}{m} \right)^{-1/4} = \sqrt{\frac{\delta}{c} / \sqrt{\frac{4\pi q^2 n}{m}}}$$

However it is when we take the inductive back-emf into account that we can improve matters.

Now, for Implicit Midpoint,

$$J_{k+1} += \frac{h \frac{q^2 n}{m}}{1 - ... + \pi h^2 \frac{q^2 n}{m}} \nabla \phi_{k+1/2}$$

This means that when we consider the effect of $\frac{\partial \phi}{\partial t}$ on J_{k+1} it is controlled by that division:

$$\left(h^4 \frac{c^2}{\delta^2} \frac{4\pi q^2 n}{m} \right) / \left(\pi h^2 \frac{q^2 n}{m} \right) = h^2 4 \frac{c^2}{\delta^2}$$

so that the critical timestep MIGHT become $h < \delta / (2c)$.

This idea was tested for a 1-dimensional ring of cells, with offset velocity, **and was found to work**.

3.3 What now

Getting stability

Naturally, solving an ODE for implicit charge flow creates a runtime cost that is prohibitive at the timestep where light crosses a cell. Therefore there are two possible ways forward:

(i) Accept that the timestep must be substantially lower than the plasma period. Still use a careful method such as IMV.

(ii) Relying on the above heuristic, see whether stability can be obtained from IMV only respecting the timestep $\delta/2c$.

The effectiveness of idea (ii) has been tested on a 1-dimensional ring of cells and found to work in that case. Clearly, the plasma period is not drastically less than the light propagation timestep anyway, so this is not crucial. But we do also know that just being within the plasma period, there are basic RK methods that will not succeed - this can be easily tested for a 1D harmonic oscillator which is equivalent.

Therefore basically we will want a method that looks something like the IMV method described above, but it is not clear how easy it will be to get the timestep up to $\delta/2c$.

Onset versus offset

An implementation based on having n, v, T on vertices did not succeed. The result of the program was an oscillating patchwork of potential, current and charge. This could well be because a change in ρ and hence ϕ at a location has an effect that is distributed through the surrounding data points instead of the effect falling essentially on ρ at the location itself. This idea is cognate with the situation for

a Jacobi iteration for a linear equation, where diagonal dominance ensures convergence. Also with the situation where a hydrodynamic simulation involving thermal pressure can result in locked chequerboard configurations that are not realistic, unless velocity is offset.

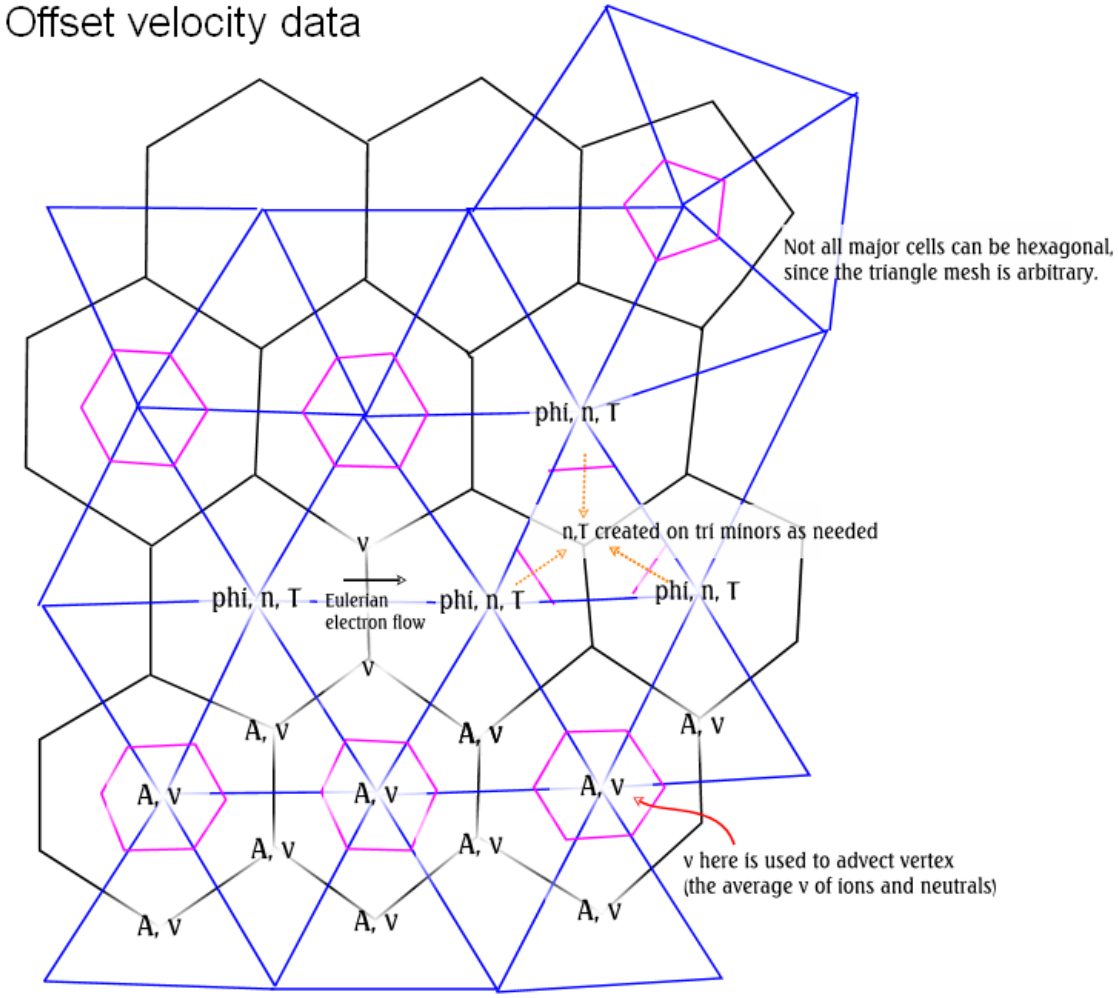

Here, we hope that offsetting electron velocity (and other species velocity relative to the mesh) will allow sensible results by allowing each ϕ value to primarily affect the ρ that directly affects that ϕ. Offsetting velocity is awkward, because with an arbitrary set of data locations, it is not possible to form two hexagonal meshes offset from each other: not all the vertex-centered cells are hexagonal. The intention is shown in the diagram: ϕ, n, T are stored only on vertices but A, v are stored on both triangles and vertices. There are thus 3 times as many A, v values as ϕ, n, T values, which does seem a bit peculiar.

We do not put A, v just on triangles because we need to take ∇v and ∇A over each edge, and so desire the honeycomb property that 3 edges meet at every corner. Therefore we create a minor mesh by slicing off the corners of the triangles and forming "central" cells. Although A could be defined at triangle circumcenters in order to avoid the need for a vector estimate of ∇A on edges, this has its own foible that circumcenters can end up very close together, so it's not a good way on the whole.

To get a bit more symmetry, it is possible to imagine actually storing n, T to represent the mass and heat in each triangle, and allowing that species relative velocity at the corners can be used to compute boundary flows through triangle edges. For now it is assumed that we simply average to triangle centres to infer n, T there when values are needed.

It is worth noting that for the toy model with a 1D ring of cells, where it was found that $\delta/2c$ could be a viable timestep, there was offset velocity.

Status quo

The onset-data program established that a manageable runtime could apparently be attained with this approach using a modest graphics card.

If this simulation fails by producing similar results to the previous program, then it will be because

the charge oscillation instability is not quite overcome by the implicit treatment of Faraday. In this case I would attempt a method based on a fixed number of iterations to create the advance for ϕ, which will be more logical in the context of offset v data. (If that fails then it is hard to argue that an ODE-solving approach can compete with dropping the timestep 10 times and being reduced to an explicit approach, careful enough that it does not explode.)

The following figure describes the procedure for 1 simulation step:

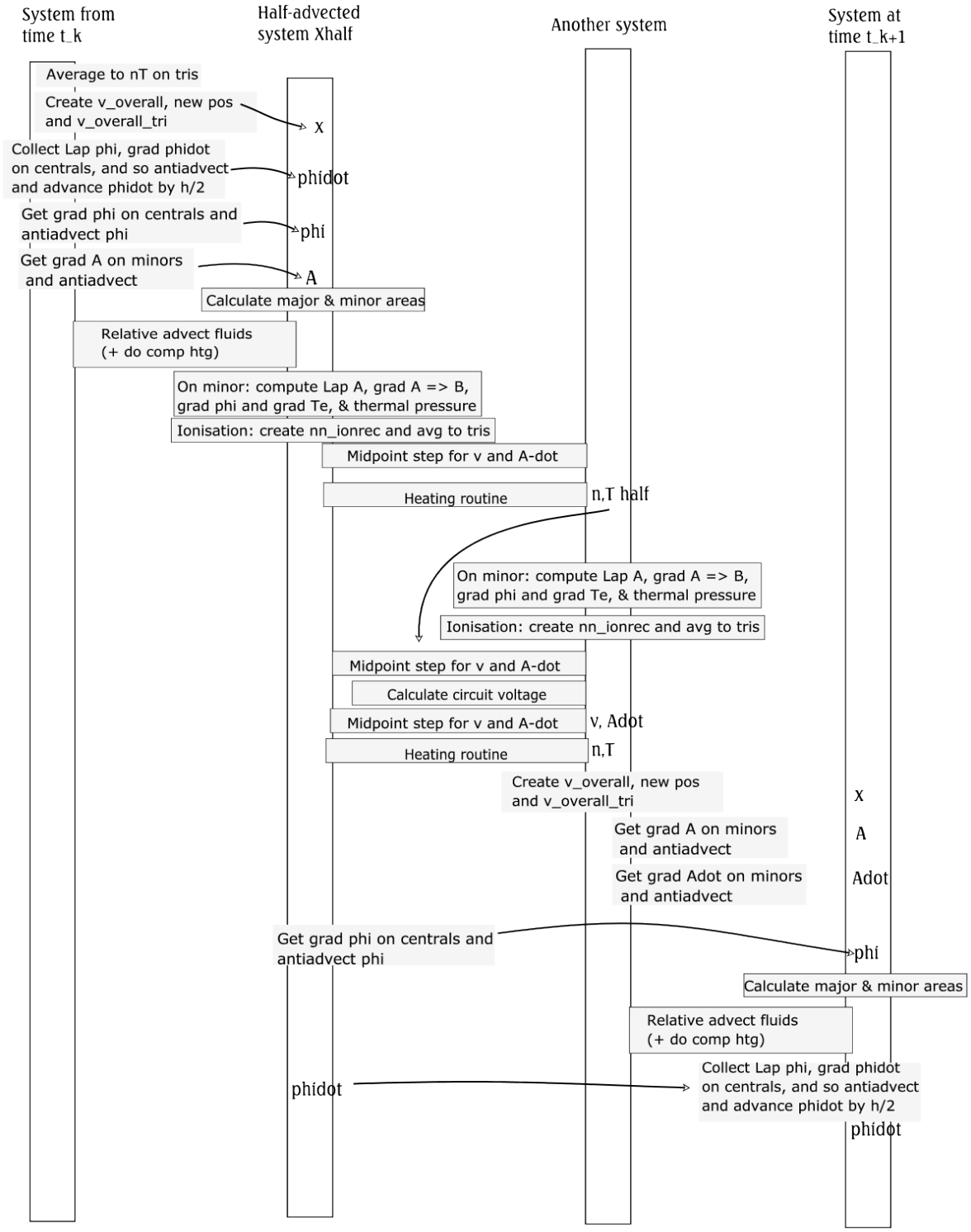

Some of the labels require a little explanation:

$$v_{overall} = \frac{m_n n_n v_n + m_i n_i v_i + m_e n_e v_e}{m_n n_n + m_i n_i + m_e v_e}$$

is the vertex advection velocity. It can be averaged on to triangles (the centre of the triangle is moved with the simple average of corner velocities, clearly) so that we can there work out the relative species velocities.

Fields have to be anti-advected because the mesh is moving but there is no reason for them to be carried along with it. This unfortunately is a bit troublesome.

Compressive heating is based on the area change of the cell containing mass and heat.

nn_ionrec is the data about the amounts of density that are ionising and recombining.

The circuit applied E_z field strength can only be calculated once the midpoint routine has been run to predict, for the final set of inputs, a linear equation for the total current I_z.

References

[GZS1977] V.E. Golant, A.P. Zhilinskii, I.E. Sakharov. Fundamentals of Plasma Physics. 1977 (English translation 1980, Wiley).

[EpperleinHaines1986] E.M. Epperlein, M.G. Haines. Plasma transport coefficients in a magnetic field by direct numerical solution of the Fokker-Planck equation. Physics of Fluids 29, issue 4 (1986)

[BL91] C.K. Birdsall, A.B. Langdon. Plasma Physics via Computer Simulation. (IoP series in plasma physics) Taylor and Francis, 2005 (hardback 1991).

[NRLFormulary] D. Book, J. D. Huba. NRL Plasma Formulary. 2009.

[Hewett1985] D. W. Hewett. Elimination of electromagnetic radiation in plasma simulation: the Darwin or magnetoinductive approximation. Space Science Reviews 42,1. pp 29-40. 1985.

[Braginskii1965] S.I.Braginskii, Transport Processes In a Plasma. 1965.